Materials Research. 2016; 19(6): 1351-1355
DOI: http://dx.doi.org/10.1590/1980-5373-MR-2015-0683

Synthesis of Star-Shaped Lead Sulfide (PbS) Nanomaterials and theirs Gas-Sensing Properties

Chengwen Song[a]*, Menghan Sun[a], Yanyan Yin[a], Jingkun Xiao[a], Wei Dong[a], Chen Li[a], Li Zhang[a]

[a] *College of Environmental Science and Engineering, Dalian Maritime University, 1 Linghai Road 116026, Dalian, China*

Received: November 12, 2015; Revised: August 11, 2016; Accepted: September 04, 2016

Star-shaped PbS nanomaterials are synthesized by a hydrothermal method. Morphology and structure of the PbS nanomaterials are analyzed by SEM, HRTEM and XRD. Gas-sensing properties of the as-prepared PbS sensor are also systematically investigated. The results show star-shaped PbS nanostructure consists of four symmetric arms in the same plane and demonstrate good crystallinity. With the increase of ethanol concentration, the sensitivity of the PbS sensor significantly increases and demonstrates an almost linear relationship at the optimal operating temperature of 400 °C. Moreover, the fast response-recovery towards ethanol is also observed, which indicates its great potential on ethanol detection.

Keywords: *Preparation; Nanomaterials; Ethanol; Gas sensor*

1. Introduction

The leak of flammable, toxic and explosive gases in industrial processes will cause serious environmental and safety problems[1]. Many traditional detection methods, such as gas chromatography, mass spectrometers, and optical spectroscopy etc., have been used for the accurate quantification of these gases. However, the use of these techniques often requires expensive and bulky instruments, skilled operators and tedious sample preparation processes. Therefore, the design of miniaturized smart sensors for fast and real-time detection has become an important and urgent strategy in the modern industrial production[2,3].

Up to date, several types of gas sensors, including semiconductor gas sensors, liquid electrolyte gas sensors, solid electrolyte gas sensors and catalytic combustion gas sensors etc., have been developed for commercial applications[4]. A number of gas-sensing materials, such as semiconductor, intrinsically conducting polymer, conducting polymer composite etc. have been adopted in these sensors based on various transduction units, for example, chemiresistive, surface acoustic wave, quartz crystal microbalance, optical transducers and metal-oxide-semiconductor field-effect transistor (MOSFET)[5]. Among them, chemiresistive gas sensors based on semiconductor have been subjected to extensive research and development due to their advantageous features such as low cost, high sensitivity, fast response/ recovery time, and simplicity in device structure and circuitry[6].

With the fast development of nanotechnology, many nanosized semiconductors, including SnO_2, ZnO, ZnS, WO_3, TiO_2 etc., have been fabricated and employed as gas sensors[7]. Lead sulfide (PbS) is an important IV–VI semiconductor with a narrow band gap energy (0.41eV) and large excition Bohr radius (18 nm), And it has been widely studied in many fields, such as solar cells, IR photodetectors and display devices etc.[8]. As previous report, nanosized semiconducting materials usually exhibit a wide range of electrical and optical properties that depend sensitively on both morphologies and sizes[9]. Hence, much attentions have been paid on synthesis of a variety of PbS nanostructures, such as nanoparticles[10], quantum dots[11], nanorods[12], nanobelts[13] nanowires[14], cubes[15], dendrites[16], star-like[17] and hierarchical structures[18] etc. Although we always stress that the morphology and size of nanomaterials significantly affect their properties, the internal relationship is not yet clear and still needs to be investigated for the further development of high-performance electrical and optical devices[19]. Recently, PbS nanomaterials have been successfully applied as promising candidates for fabricating gas sensors by a few research groups. Markov and Maskaeva reported their works on PbS films used for nitrogen oxides detection[20]. Shimizu et al. fabricated the metal-mono sulfide based (NiS, CdS, SnS and PbS) solid electrolyte sensors, and found their good SO_2 sensitivity[21,22]. Kaci et al. synthesized PbS thin films by modified polyol process on amorphous a-SiC and p-Si(100) substrates, which exhibited highly sensitive with fast response to H_2 [23]. Fu obtained PbS sensors with high responses to NO_2 and NH_3 [24].

Ethanol detection are great important in many fields including control of fermentation processes, safety testing of food packaging, and monitoring drunken driving etc.[25]. However, to the best of our knowledge, there is not any study about the detection of ethanol gas using PbS gas sensors. In this work, we synthesized star-shaped PbS nanomaterials using a simple hydrothermal method, investigated their morphologies and structure characteristics, and further assess their gas sensing properties and potential in ethanol detection.

* e-mail: chengwensong@dlmu.edu.cn

2. Experimental

2.1. Preparation of PbS nanomaterials

3.2 mmol of $Pb(Ac)_2 \cdot 3H_2O$ (CAS number: 6080-56-4) and 80 mmol thiourea (CAS number: 62-56-6) were added to 80 mL of deionized water under stirring. The mixture was sealed in a Teflon-lined stainless steel autoclave of 100 mL capacity and heat at 170 °C for 12 h, and then cooled to room temperature. The resulting precipitates were collected by centrifugation and washed three times by deionized water and ethanol (CAS number: 64-17-5) to remove possible impurities, and subsequently dried at 60 °C for 10 h.

2.2. Characterizations

X-ray diffraction (XRD) patterns of PbS nanomaterials were recorded using a D/Max-2400 diffractometer (Cu Kα radiation, λ =1.54055Å) in a range of diffraction angle 2θ from 10° to 80° to analyze the diffraction peaks of PbS. The morphologies of PbS nanomaterials were observed by a scanning electron microscope (SEM) (Philips XL30 FEG) and a high-resolution transmission electron microscopy (HRTEM) (FEI/Philips Techal 12 BioTWIN).

2.3. Fabrication and measurement of PbS gas sensor

PbS nanomaterials were mixed with several drops of ethanol to form a slurry, and then the slurry was brush-coated onto the surfaces of an alumina tube with two Au electrodes and four Pt wires. A Ni–Cr heating wire was inserted into the alumina tube and used as a heater. The alumina tube was then welded onto a pedestal with six probes to obtain the final sensor unit. Gas sensing tests were performed on a WS-30A static gas-sensing system (HanWei Electronics Co., Ltd., Henan, China) using ambient air as the dilute and reference gas, which is operated at the controllable ambient temperature (25 ± 1 °C) and relative humidity (~ 30 ± 5 % RH). A typical testing procedure is presented as follows:

Firstly, the PbS sensor is put into the test chamber (18 L in volume). After the resistance of the PbS sensor is stable, the calculated amount of tested solution is manually injected into the test chamber by a microsyringe, and then, the tested solution is evaporated by a quick evaporator and mixed with air immediately by two installed fans, which constitutes the measurement atmosphere. Afterwards, the test chamber is opened and the PbS sensor begins to recover in air[26,27].

The sensor sensitivity is defined as follows,

$$Sensitivity = \frac{R_a}{R_g}$$

where R_a and R_g are the electrical resistance of the sensor in air and in test gas, respectively.

3. Results and discussion

3.1. Morphology and Structure of PbS nanomaterials

The phase composition and structure of the synthesized product are investigated by XRD. Figure 1 demonstrates the representative XRD pattern of the as-prepared product, which show the diffraction peaks at 2θ values 26.09°, 30.19°, 43.17°, 51.09°, 53.52°, 62.64°, 68.98°, 71.04° and 79.27°. All the diffraction peaks are assigned to (111), (200), (220), (311), (222), (400), (331), (420), and (422) planes of a face-centered-cubic structured PbS (JCPDS No. 05-592), and no other peaks are observed, suggesting pure PbS is obtained[28]. The sharp and strong intensity of XRD peaks suggest that the samples have high crystallinity. The morphology of the PbS nanomaterials are observed by SEM and TEM images. As shown in Figure 2a. The PbS nanomaterials show the morphology of star-shaped nanostructures. All the products observed exhibit similarities in shape and morphology but slightly varied in size. TEM image reveals that individual star-shaped PbS nanostructure consists of four symmetric arms in the same plane extend radially from the center (Figure 2b). From the HRTEM image of the PbS sample (Figure 2c), it can be seen that the fringe spacing of pure PbS is about 0.295 nm, which corresponding to the interplanar spacing of (200) planes of the face-centered-cubic structured PbS[9].

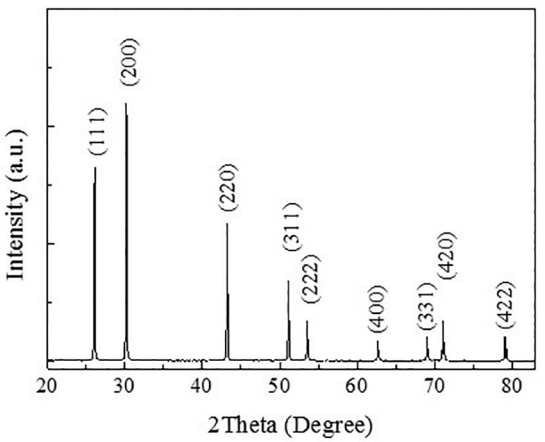

Figure1: XRD patterns of PbS sample.

3.2. Gas sensing properties of PbS nanomaterials

Operating temperature plays an important role in determining the response of the sensor to ethanol. Figure 3 present the sensitivity of the PbS sensor towards 100 ppm ethanol at various operating temperature. It is obvious that the PbS sensor demonstrate the increasing sensitivity with the increase of the operating temperature and reaches

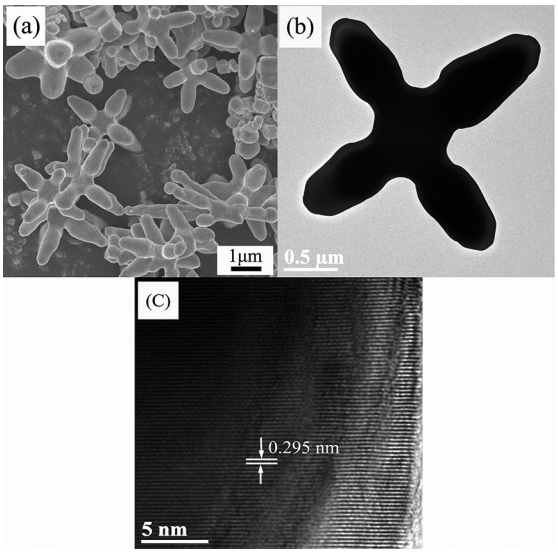

Figure 2: (a) SEM, (b) TEM, and (c) HRTEM images of PbS.

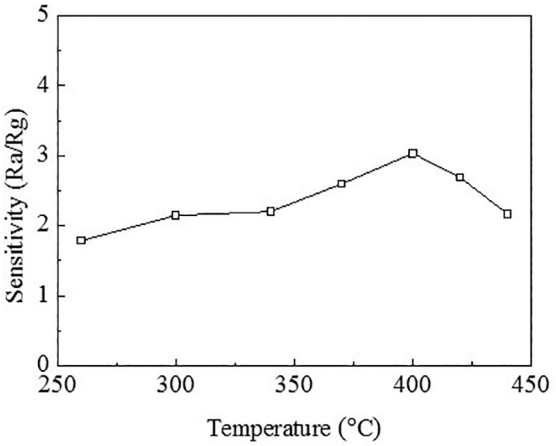

Figure 3: Sensitivity of the PbS sensor at different operating temperatures

a maximum of 3.04 at 400 °C, and then decreases. The phenomenon can be explained by the fact that it is hard for ethanol molecules to react with adsorbed oxygen species (O^-, O_2^-, O^{2-}) at lower operating temperature due to insufficient thermal energy, while higher operating temperature makes the adsorbed oxygen species (O^-, O_2^-, O^{2-}) reduce and thus limits gas response towards ethanol molecules[29]. Therefore, the optimal operating temperature is 400 °C for the PbS sensor.

Figure 4 displays a variation between the sensitivity of the PbS sensor and ethanol concentration from 10 ppm to 300 ppm at operating temperature of 400 °C. As observed, the detection limit of the PbS sensor toward ethanol is 10 ppm. With the increase of ethanol concentration, the sensitivity of the PbS sensor significantly increases and demonstrates an almost linear relationship between them. The response and recovery times are also an important parameter to assess the gas-sensing property of the PbS sensor. Figure 5 provides

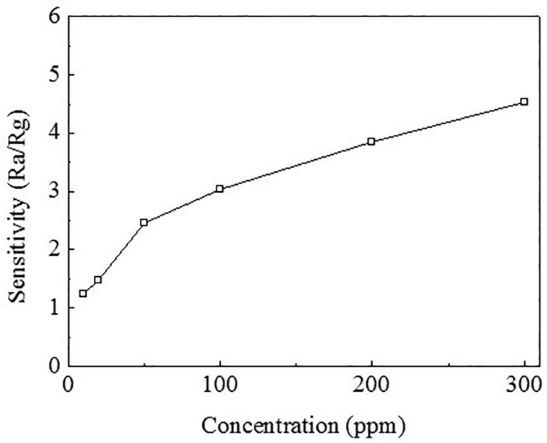

Figure 4: Sensitivity of PbS sensor to different ethanol concentrations.

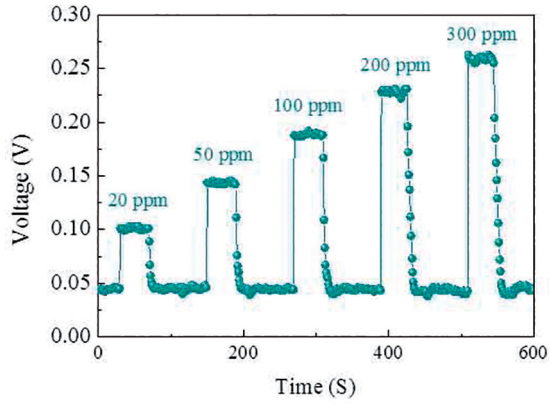

Figure 5: Response-recovery curves of the PbS sensors to different ethanol concentrations.

the response-recovery curves of the PbS sensor towards ethanol with different concentrations at operating temperature of 400 °C. Generally, the times to reach 90 % variation in resistance upon exposure to ethanol and air are defined as the 90 % response time ($t_{response}$) and the 90 % recovery time ($t_{recovery}$), respectively. As observed, the PbS sensor exhibits fast response and recovery to 20, 50, 100, 200, and 300 ppm ethanol. The response times are all less than 1 s and the recovery time upon exposure to 20, 50, 100, 200, and 300 ppm ethanol are 6 s, 7 s, 9 s, 10 s and 11 s, respectively. The fast response and recovery speed suggests that the diffusion of ethanol and its oxidation by oxygen species (O^-, O_2^-, O^{2-}) are very rapid in the star-shaped structure.

3.3. Gas-sensing mechanism of PbS sensor

The gas-sensing mechanism of the PbS sensor towards ethanol can be interpreted by the interaction between ethanol molecules and the absorbed oxygen species (O^-, O_2^-, O^{2-}) on the surface of the PbS sensor[30]. Generally, the type of

absorbed oxygen species is determined by the operating temperature, and O^{2-} becomes the main form of oxygen species at the operating temperature of 400 °C[31]. When the PbS sensor contacts with the air, oxygen molecules in the air will adsorb on the surfaces of the PbS sensor and trap electrons from the conduction band of the PbS sensor, forming oxygen species (O^-, O_2^-, O^{2-}) (Eqs.(1)-(4)), which results in the formation of the electron depletion layer on the surface of the PbS sensor and makes the resistance of the PbS sensor increase. As ethanol is introduced into the system, ethanol molecules will react with the oxygen species (O^-, O_2^-, O^{2-}) adsorbed on the surface of the PbS sensor, thus the captured electrons are released back to conduction band of the PbS sensor, which leads to a decreased resistance (Eqs.(5)-(7)).

$$O_2(gas) \rightarrow O_2(ads) \quad (1)$$

$$O_2(ads) + e^- \rightarrow O_2^-(ads) \quad (2)$$

$$O_2^-(ads) + e^- \rightarrow 2O^-(ads) \quad (3)$$

$$O^-(ads) + e^- \rightarrow O^{2-}(ads) \quad (4)$$

$$C_2H_5OH(gas) \rightarrow C_2H_5OH(ads) \quad (5)$$

$$C_2H_5OH(ads) + 6O^-(ads) \rightarrow 2CO_2(gas) + 3H_2O(gas) + 6e^- \quad (6)$$

$$C_2H_5OH(ads) + 6O^{2-}(ads) \rightarrow 2CO_2(gas) + 3H_2O(gas) + 12e^- \quad (7)$$

4. Conclusions

In summary, we have synthesized star-shaped PbS nanomaterials using a simple hydrothermal method. The sensitivities of the as-prepared PbS sensor towards 100 ppm ethanol increase with operating temperature and then reach a maximum, The PbS sensor reveals fast response and recovery time for the detection of ethanol concentration in the range of 10–300 ppm at the optimal operating temperature of 400 °C. The gas-sensing mechanism of the PbS sensor towards ethanol can be interpreted by the interaction between ethanol molecules and the absorbed oxygen species (O^-, O_2^-, O^{2-}) on the surface of the PbS sensor.

5. Acknowledgement

This work was supported by the Scientific Research Project of Education Department of Liaoning Province (L2013203), The Natural Science Foundation of Liaoning Province (2014025014), the Fundamental Research Funds for the Central Universities (3132016327), the Scientific Public Research Foundation of Liaoning Province (2013003007), the Science and Technology Foundation for Overseas Chinese Scholars, Ministry of Human Resources and Social Security of China, and the National Natural Science Foundation of China (21276035, 21476034).

6. References

1. Samerjai T, Tamaekong N, Wetchakun K, Kruefu V, Liewhiran C, Siriwong C, et al. Flame-spray-made metal-loaded semiconducting metal oxides thick films for flammable gas sensing. *Sensors and Actuators B: Chemical*. 2012;171-172:43-61.

2. Fan F, Tang P, Wang Y, Feng Y, Chen A, Luo R, et al. Facile synthesis and gas sensing properties of tubular hierarchical ZnO self-assembled by porous nanosheets. *Sensors and Actuators B: Chemical*. 2015;215:231-240.

3. Wei F, Zhang H, Nguyen M, Ying M, Gao R, Jiao Z. Template-free synthesis of flower-like SnO_2 hierarchical nanostructures with improved gas sensing performance. *Sensors and Actuators B: Chemical*. 2015;215:15-23.

4. Hsu C, Tsai J, Hsueh TJ. Ethanol gas and humidity sensors of CuO/Cu_2O composite nanowires based on a Cu through-silicon via approach. *Sensors and Actuators B: Chemical*. 2016;224:95-102.

5. Wetchakun K, Samerjai T, Tamaekong N, Liewhiran C, Siriwong C, Kruefu V, et al. Semiconducting metal oxides as sensors for environmentally hazardous gases. *Sensors and Actuators B: Chemical*. 2011;160(1):580-591.

6. Yamazoe N, Shimanoe K. New perspectives of gas sensor technology. *Sensors and Actuators B: Chemical*. 2009;138(1):100-107.

7. Comini E. Metal oxide nano-crystals for gas sensing. *Analytica Chimica Acta*. 2006;568(1-2):28-40.

8. Salavati-Niasari M, Ghanbari D, Loghman-Estarki MR. Star-shaped PbS nanocrystals prepared by hydrothermal process in the presence of thioglycolic acid. *Polyhedron*. 2012;35(1):149-153.

9. Ao D, Ichimura M. UV irradiation effects on hydrogen sensors based on SnO_2 thin films fabricated by the photochemical deposition. *Solid-State Electronics*. 2012;69:1-3.

10. Mamiyev ZQ, Balayeva NO. Preparation and optical studies of PbS nanoparticles. *Optical Materials*. 2015;46:522-525.

11. Yang Y, Wang W. Effects of incorporating PbS quantum dots in perovskite solar cells based on $CH_3NH_3PbI_3$. *Journal of Power Sources*. 2015;293:577-584.

12. Yousefi R, Cheraghizade M, Jamali-Sheini F, Basirun WJ, Huang NM. Effect of hydrogen gas on the growth process of PbS nanorods grown by a CVD method. *Current Applied Physics*. 2014;14(8):1031-1035.

13. Zhou SM, Zhang XH, Meng XM, Fan X, Lee ST, Wu SK. Sonochemical synthesis of mass single-crystal PbS nanobelts. *Journal of Solid State Chemistry*. 2005;178(1):399-403.

14. Wang Z, Zhao B, Zhang F, Mao W, Qian G, Fan X. Novel single-crystal PbS nanowires directed by [200]. *Materials Letters*. 2007;61(17):3733-3735.

15. Sun SS, Han QF, Wu XD, Zhu JW, Wang X. The facile synthesis of PbS cubes and Bi_2S_3 nanoflowers from molecular precursors at room temperature. *Materials Letters*. 2011;65(21-22):3344-3347.

16. Devi PI, Sivabharathy M, Ramachandran K. Enhancement of dielectric constant in PVDF polymer using dendrite-shaped PbS nanostructures. *Optik - International Journal for Light and Electron Optics*. 2013;124(19):3872-3875.

17. Salavati-Niasari M, Ghanbari D. Hydrothermal synthesis of star-like and dendritic PbS nanoparticles from new precursors. *Particuology*. 2012;10(5):628-633.

18. Mocanu A, Rusen E, Diacon A, Dinescu A. Hierarchical nanostructures of PbS obtained in the presence of water soluble polymers. *Powder Technology*. 2014;253:237-241.

19. Li G, Li C, Tang H, Cao K, Chen J. Controlled self-assembly of PbS nanoparticles into macrostar-like hierarchical structures. *Materials Research Bulletin*. 2011;46(7):1072-1079.

20. Markov VF, Maskaeva LN. Lead Sulfide Semiconductor Sensing Element for Nitrogen Oxide Gas Analyzers. *Journal of Analytical Chemistry*. 2001;56(8):754-757.

21. Souda N, Shimizu Y. Sensing properties of solid electrolyte SO_2 sensor using metal-sulfide electrode. *Journal of Materials Science*. 2003;38(21):4301-4305.

22. Shimizu Y, Okimoto M, Souda N. Solid-State SO_2 Sensor Using a Sodium-Ionic Conductor and a Metal–Sulfide Electrode. *International Journal of Applied Ceramic Technology*. 2006;3(3):193-199.

23. Kaci S, Keffous A, Hakoum S, Mansri A. Hydrogen sensitivity of the sensors based on nanostructured lead sulfide thin films deposited on a-SiC:H and p-Si(100) substrates. *Vacuum*. 2015;116:27-30.

24. Fu T. Research on gas-sensing properties of lead sulfide-based sensor for detection of NO_2 and NH_3 at room temperature. *Sensors and Actuators B: Chemical*. 2009;140(1):116-121.

25. Rao P, Godbole RV, Bhagwat S. Nanocrystalline Pd:$NiFe_2O_4$ thin films: A selective ethanol gas sensor. *Journal of Magnetism and Magnetic Materials*. 2016;416:292-298.

26. Tan W, Yu Q, Ruan X, Huang X. Design of SnO_2-based highly sensitive ethanol gas sensor based on quasi molecular-cluster imprinting mechanism. *Sensors and Actuators B: Chemical*. 2015;212:47-54.

27. Han B, Liu X, Xing X, Chen N, Xiao X, Liu S, et al. A high response butanol gas sensor based on ZnO hollow spheres. *Sensors and Actuators B: Chemical*. 2016;237:423-430.

28. Phuruangrat A, Thongtem T, Kuntalue B, Thongtem S. Characterization of cubic and star-shaped dendritic PbS structures synthesized by a solvothermal method. *Materials Letters*. 2012;81:55-58.

29. Chen W, Zhou Q, Wan F, Gao T. Gas Sensing Properties and Mechanism of Nano-SnO_2-Based Sensor for Hydrogen and Carbon Monoxide. *Journal of Nanomaterials*. 2012;2012:612420.

30. Jin W, Yan S, An L, Chen W, Yang S, Zhao C, et al. Enhancement of ethanol gas sensing response based on ordered V_2O_5 nanowire microyarns. *Sensors and Actuators B: Chemical*. 2015;206:284-290.

31. Li Z, Huang Y, Zhang S, Chen W, Kuang Z, Ao D, et al. A fast response & recovery H_2S gas sensor based on α-Fe_2O_3 nanoparticles with ppb level detection limit. *Journal of Hazardous Materials*. 2015;300:167-174.